DOI: https://doi.org/10.14311/TPFM.2025.013

NEBULIZER BASED DEVICES FOR FINE NANOPARTICLE COATING

J. Hájek, M. Malý, O. Cejpek, J. Jedelský

Energy Institute, Faculty of Mechanical Engineering, Brno University of Technology, Technicka 2896/2, 616 69 Brno, Czech Republic

Abstract

Spray coating is one of the most affordable methods for creating thin layers of material on the surface of various objects. However, as the desired coating height decreases, the application process needs to be more precisely controlled. In this study, an ultrasonic nebulizer-based spray coating device was developed. This device allows atomization of various nanofluids, including those containing nanoparticles, and enabling variation of their impact velocity. Spray characteristics were measured using Doppler anemometry (PDA) in three axial locations. The atomized nanofluids included water- and ethanol-based solutions with nanodiamonds and TiO_2 concentrations of 10 and 1 mg/ml. Measurement data revealed that the device effectively produced a narrow droplet size spectrum (with most droplets below 5 μm), controlled their velocity (ranging from 20 to 138.1 m·s⁻¹). Desired droplet deposition regime was achieved with nebulizer-based spray device.

Keywords: spray coating, mesh nebulizer, Phase Doppler anemometry

1 Introduction

Nanoparticle coatings are used across a wide range of applications, such as medicine[1, 2], agriculture [3, 4] or electronic [5, 6]. Many methods, including dip coating, spin coating, spray coating or blade coating are employed to form a thin layers of nanoparticles (NP). Each technique offers unique advantages, but the spray coating method stands out for its high material efficiency, layer thickness control, and scalability for industrial applications [7].

The spray coating process consists of the atomization of a NPs solution into small droplets, their transport onto the object surface, droplets/surface interactions, and droplets evaporation, which leads to NPs deposition. All stages of the process significantly affect the coating structure. The role of atomization is to create a fine spray of droplets with uniform size and sufficient kinetic energy to reach the surface of the coated object. Various techniques can be used for atomization, such as hydraulic or pneumatic atomization, ultrasonic atomization, or atomization by electrical forces. Due to the significant decrease in droplet velocity with increasing distance from the nozzle in certain atomization techniques, additional mechanisms are needed to increase droplet velocity. One of the simplest mechanisms is to impart velocity to the droplets using high-velocity air or gas.

The droplet-surface interaction is influenced by the droplet size, velocity, the liquid rheology, and the surface properties. Different contact regimes can occur when a droplet interacts with a surface. Naber and Farrell [8] determined the spread and splash regimes based on the Weber number (*We*):

$$\boldsymbol{We} = \frac{\boldsymbol{v^2 \cdot D \cdot \rho}}{\boldsymbol{\sigma}} \tag{1}$$

where v is droplet velocity, D is mean droplet diameter, ρ is liquid density and σ is liquid surface tension. In the spread regime, the droplet forms a thin liquid film upon interacting with the surface. This behaviour occurs when $We < 130$. When $We > 130$ the splash regime develops. In this regime, the droplet has sufficient kinetic energy to overcome surface tension forces, resulting in secondary atomization. It should be noted that this behaviour was determine based on wetted wall-droplet interaction and relatively large droplets with a diameter of 3.4 mm. Mundo et al [9]. focused on much smaller droplets from 60 to 150 μm in diameter and their interaction with dry wall. The boundary between the spread (or deposition) and splash regimes was determined by the critical parameter K, expressed as follows:

$$\boldsymbol{K = Oh \cdot Re^{1,25}} \tag{2}$$

where

$$\boldsymbol{Oh} = \frac{\boldsymbol{\mu}}{\sqrt{\boldsymbol{\rho \cdot \sigma \cdot D}}} \tag{3}$$

$$\boldsymbol{Re} = \frac{\boldsymbol{\rho \cdot v \cdot D}}{\boldsymbol{\mu}} \tag{4}$$

where *Oh* is the Ohnesorge number, *Re* is the Reynolds number and μ is the liquid dynamic viscosity. The spread regime occurs when $K < K_{lim}$. The K_{lim} was determined to be 57.7 [9]. When $K > K_{lim}$, the splash regime develops. Rioboo et al. [10] expanded on this topic by focusing on the influence of the surface. A total of six contact regimes were introduced, along with the parameters that affect them. These contact regimes - deposition, prompt splash, receding breakup, complete breakup, corona splash, and partial rebound - were defined. The effect of parameters v, D, σ, μ, roughness amplitude (R_a), roughness wavelength (R_w) and contact angle (θ) on the contact regimes were determined. Based on [10], it is evident that surface characteristics must also be considered when determining the contact regime.

Ensuring the correct contact regime is essential when designing a spray coating device, regardless of the nanofluid or surfaces being used. The preferable contact regime is the spread/deposition regime, as it allows the droplet to cover the largest area and promotes intense evaporation. On the other hand, when the nanofluid is pre-atomized and the droplets are accelerated by the high-pressure gas, the rebound regime on the device's internal walls is desirable. The rebound regime reduces nanofluid settling inside the device, prevents clogging, and avoids the formation of larger droplets, which could negatively impact coating thickness and structure.

The aim of the most NP coatings is to achieve homogeneous deposition of primary droplets without agglomerates. In the spray coating process, agglomeration is influenced primarily by σ [11], μ [12], and D [13]. The σ and μ are determined by the rheology of the nanofluid, D is determined by the atomization process. As droplet size increases, agglomeration becomes more significant [13], therefore, atomizing the nanofluid into droplets just a few microns in diameter is essential.

Droplet interaction with the surface phenomena must be considered, when designing the spray device. In the works of Rukosuyev [14] and Franke [15] spray devices for forming thin NP coatings were presented. In both studies, the nanofluids were pre-atomized and then accelerated using compressed gas. This approach enables adjustment of droplet speed to achieve the desired contact regime. In both cases, uniform droplets were produced via ultrasonic atomization. A device based on ultrasonic nebulizer with 1.65 MHz piezoelectric element was used in Rukosuyev. The spray apparatus developed by Franke contained the membrane vibrating at 113 kHz which allows for aerosol forming. Both devices produced a fine spray with droplets between 2.5 to 6 μm. Both studies achieved NP coatings with thicknesses below 1 μm, due to the ability to adjust the droplet impact speed.

The objective of this study is to introduce a new spray coating device capable of forming a homogeneous material layer without particle agglomerates. The design is based on previous spray coating devices and the necessity to ensure the correct contact regime. Additionally, the device has to accommodate different types of nanofluids and be suitable for large-scale spray coating.

2 Experimental setup

Spray coating device was tested at the Multiphase Flow Laboratory at Brno University of Technology. A phase Doppler anemometry (PDA) system was used to determine the spray characteristics and evaluate the device's performance.

2.1 Spraying device

The spray coating device illustrated in Fig. 1 consists of a droplet generator, a cyclone-shaped chamber with an exit orifice, and a pressure gas inlet tube. Atomization is achieved using a Solo mesh nebulizer (Aerogen, IE) that incorporates a high-frequency (128 kHz) vibrating plate with 1,000 apertures. The vibrating plate forces the liquid or nanofluid through the apertures, forming a fine mist with uniform droplet size [16]. Additionally, the ultrasound waves generated by the plate may fragment NPs agglomerates in the nebulizer's liquid storage tank [17]. The nebulizer is connected to a cyclone-shaped chamber where larger droplets are captured. Droplets within the chamber are accelerated by the pressure difference created by high gas velocity at the outlet of the pressurized gas tube. A metal tube with an outer diameter of 6 mm and an inner diameter of 2.5 mm is centred along the axis using four defining elements. At the top, the tube is sealed with a rubber O-ring, allowing the position of the pressure gas inlet tube to be adjusted relative to the exit orifice. The position of the pressure gas inlet tube directly influences spray parameters, such as the spray cone angle and droplet distribution [14]. Tube's orifice and the nozzle were aligned at the same level during the experiments. The device was mounted on a linear 3D traverse system (ISEL AUSTRIA GMBH & CO. KG, AT), enabling precise movement over coated samples.

The spray device was operated at three overpressure levels: 25, 50, and 75 kPa. Compressed air was supplied from the central compressed air distribution system. The airflow rate was measured using a mass flow meter (FMA-A2100, Omega Engineering, USA) with an accuracy of ±1% of the full scale. The air mass flow rate corresponded to the air overpressure, reaching values of 2.90, 4.13, and 5.02 $kg \cdot h^{-1}$.

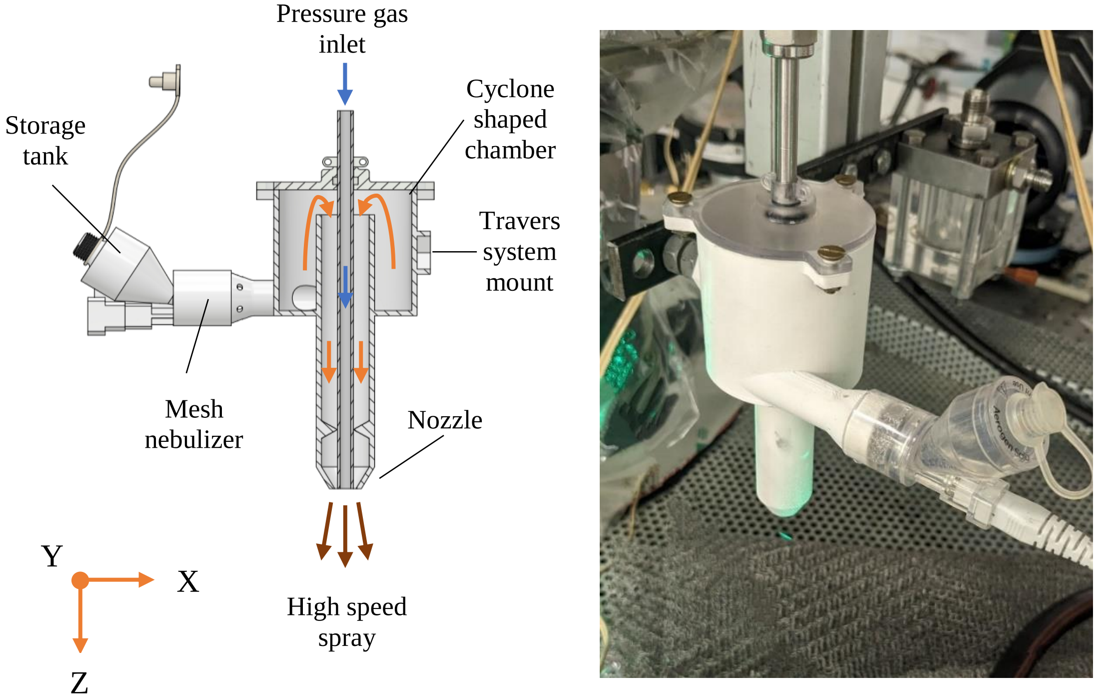

Figure 1: The spray coating device scheme (left) and model (right)

2.2 Test bench and PDA setup

The spray generated by the device was investigated on a cold test bench using a two-component Phase Doppler Anemometry (PDA) measurement system (Dantec Dynamics, DK). Droplet size and velocity were measured simultaneously, in total 94 measurement points were probed. The measurement matrix consisted of three measuring crosses at different axial distances from the nozzle outlet (see Table 1). At each point, either 25,000 droplets were measured, or a 10-second acquisition duration was reached, whichever occurred first. The PDA setup is detailed in Table 2.

It should be noted that droplets smaller than 1 µm were filtered from the original data. The accuracy of the PDA system is significantly reduced when measuring particles of this size. Repeatability was evaluated based on three measurements, with a standard deviation of 0.14 µm calculated for the average droplet size (D_{10}) 2.64 µm.

Table 1: PDA measurement probing positions

Axial distance from nozzle Z (mm)	X, Y (mm)
30	0, ±1, ±2, ±3, ±4, ±5, ±6
60	0, ±1.5, ±3, ±4.5, ±6, ±7.5, ±9, ±10.5, ±12
120	0, ±2, ±4, ±6, ±8, ±10, ±12, ±14, ±16

Table 2: PDA setup

Parameters	**Value**	
Scattering angle	68 °	
Reciever mask	Mask A	
Reciever spatial filter	0.1 mm	
Focal length of transmitting/receiving optics	500/310 mm	
Wavelength	532 nm	561 nm
Velocity component	**Axial**	**Radial**
Velocity center	212.7 $m \cdot s^{-1}$	0.0 $m \cdot s^{-1}$
Velocity span	106.4 $m \cdot s^{-1}$	112.2 $m \cdot s^{-1}$
Sensitivity	950 V	1 000 V
SNR	0 dB	0 dB
Signal gain	14 dB	18 dB
Level validation ratio	4	4

2.3 Tested solution

The device was tested using water- and ethanol-based solutions with two types of NP. Solutions of detonation nanodiamonds (ND) were prepared by the Chemical Processes and Biomaterials research group at the University of West Bohemia in Pilsen, Czech Republic. The primary ND had an average size of approximately 5 nm. Additionally, TiO2 NPs with a size of 25 nm (PlasmaChem, GmbH, DE) were used. The solutions were prepared with NP concentrations of 10 mg/ml and 1 mg/ml, based on the mass of NPs per unit volume of liquid.

3 Results and Discussion

In the following chapter the main results obtained from the experimental data are presented.

3.1 Droplet diameter

The mesh nebulizer produced a spatial homogenous droplet size distribution, as shown in Fig. 2. Based on the data, no significant difference in droplet size was observed between solutions containing different types of NPs; however, variations were noted with different NP concentrations. Solutions with higher NP concentrations were atomized into larger droplets. For ultrasonic nebulizers, the principles of droplet formation and size determination are well established as droplet size depends on the liquid's σ, ρ, and the nebulizer's excitation sound frequency [18]. In the case of a mesh grid nebulizer, the atomization process is different, relying on the exit diameter of the aperture orifices [19]. However, the data shows, that also on the rheology of liquid depend. Since, the presence of NPs effects the σ, ρ, ν [20], contact angle [21] and wettability [22], multiple measurements are necessary to determine the influence of each rheological property.

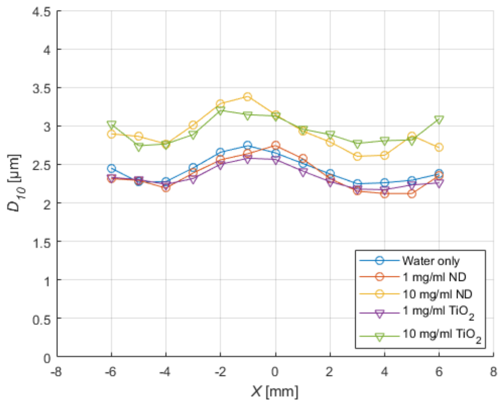

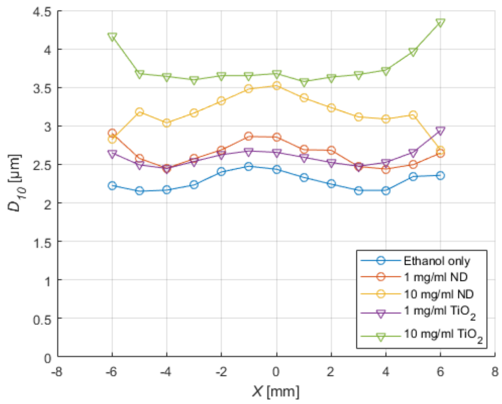

Figure 2: Droplet size across the spray, 30 mm from the nozzle orifice, air overpressure 25 kPa, water-based solution (left), and ethanol-based (right)

The Fig. 3 shows the relative frequency (*f*) of D_{10} at the center of the spray. For water and ethanol without nanoparticles, the generated droplets were under 10 µm. In all cases, more than 85% of the droplets were under 6 µm. These values align with the droplet sizes specified by the nebulizer manufacturer, suggesting that no aggregation of smaller droplets into larger ones occurs within the cyclone-shaped chamber or nozzle.

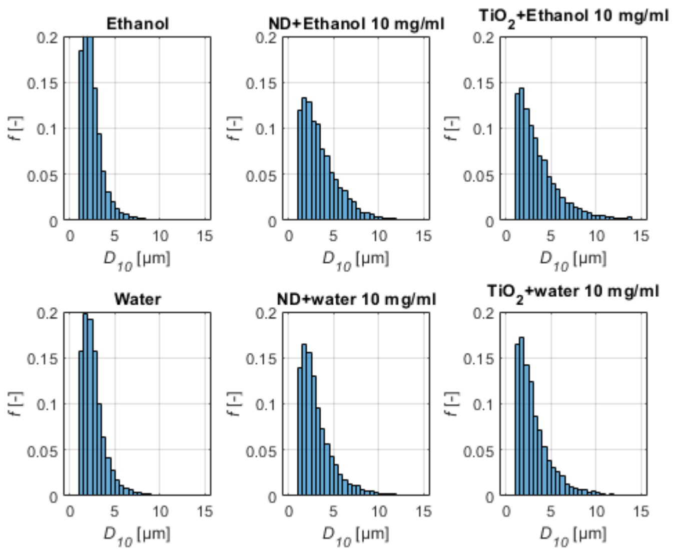

Figure 3: Droplet size distribution in spray centre, 30 mm from the nozzle orifice, air pressure 25 kPa

3.2 Velocity profile

The main goal of the velocity profile analysis was to ensure symmetry along the radial distance. If the profile were too asymmetrical, it could result in significant differences in droplet impact velocity and uneven droplet distribution across the spray. Due to the high momentum of the pressurized air, droplet size has no significant effect on droplet velocity.

The velocity profile was measured at three levels of overpressure, with droplet velocities ranging from 20 to 138.1 m·s^{-1}. Fig. 4 shows the velocity ratio as a function of the ratio between the radial distance from the spray axis and the axial distance from the nozzle orifice. The symmetry of the spray ensured that droplet velocities along the x-axis and y-axis were identical; thus, only one axis is represented in the graphs. The droplet velocity ratio varies slightly with increasing distance from the nozzle, but no discernible trend is observed. However, the velocity ratio at the same axial distance and different pressures align almost perfectly.

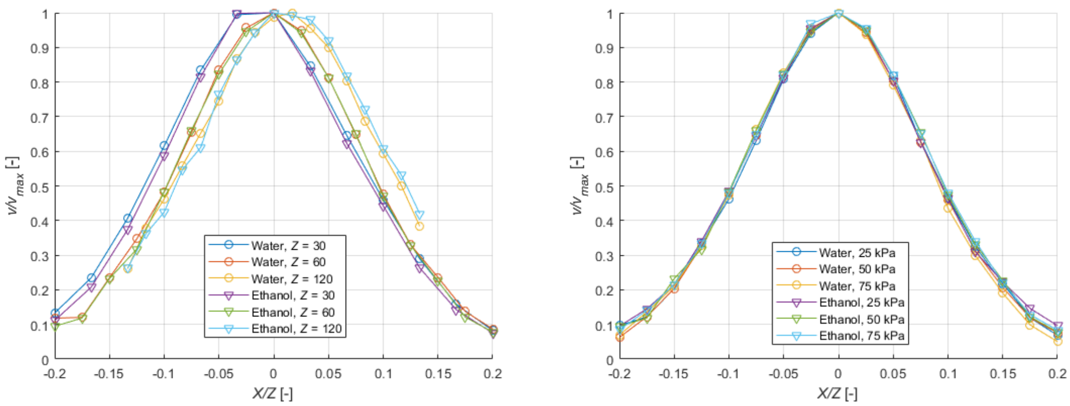

Figure 4: Droplet velocity profiles across the spray, depending on distance from nozzle orifice, 50 kPa (left) and compressed air overpressure (right), *Z* = 60 mm

3.3 Critical parameter *K*

Based on the measured droplet sizes and velocities, the critical parameter *K* was determined. The Fig. 5 presents the *K* values of ethanol and water droplets versus the axial distance from the nozzle outlet and the air overpressure together with the K_{lim}. For droplets with $K < K_{lim}$ the deposition regime occurs, which is the desired state, as it avoids splashing or rebound. However, at very low *K* values, droplets may not overcome surface forces during droplet-wall interaction and fail to form a thin film that evaporates quickly. Thus, achieving the maximum possible *K* value without transitioning into the splash regime is essential. The *K* parameter will always vary across the spray due to the velocity profile distribution. The data show that, because of differences in droplet sizes generated by water and ethanol solutions, it is necessary to adjust the air pressure for each solution depending on the coating distance. Ethanol suspensions clearly require higher air overpressures than water-based solutions at the same coating distance to achieve the desired *K*.

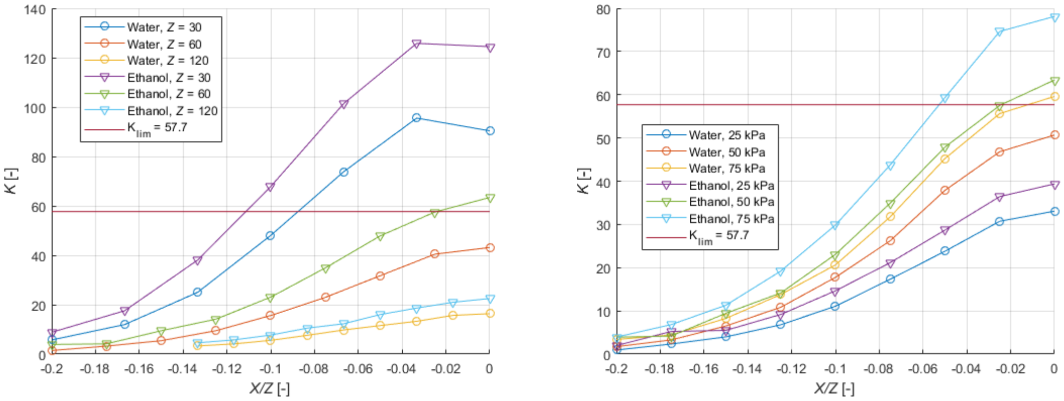

Figure 5: Critical parameter *K* depending on distance from nozzle orifice, 50 kPa (left), and compressed air overpressure (right), *Z* = 60 mm

4 Conclusion

In this work, a spray device for nanoparticle (NP) coating based on a mesh grid nebulizer is presented. The atomization capabilities of the device were tested with a total of 10 solutions, varying in NP type, concentration, and solvent base. The ability to vary droplet speed was assessed across three levels of overpressure. Spray characteristics such as droplet size and velocity were analysed using a PDA system at 96 measurement points. Smaller droplets were generated for ethanol-based solutions. However, for both solutions, there was a noticeable trend of increasing droplet size with increasing NP concentration. No significant effect of NP type on droplet size was observed. Droplet size did not vary substantially with radial distance from the spray axis, indicating uniform droplet size distribution. In contrast, the velocity profile varied significantly with radial distance, which is to be expected given the symmetry of the exit orifice and the internal nozzle arrangement. The critical parameter *K* reached higher values for ethanol, indicating that the splash mode occurred at lower overpressure levels and further from the spray axis compared to water. The device has demonstrated its ability to achieve the desired contact regime by varying air overpressure, which influences droplet velocity. It can operate effectively with a range of liquids and nanofluids.

The data that support the findings of this study are openly available at https://zenodo.org under DOI 10.5281/zenodo.15789215

Acknowledgements

Publication was supported by the project "Mechanical Engineering of Biological and Bio-inspired Systems", funded as project No. CZ.02.01.01/00/22_008/0004634 by Programme Johannes Amos Commenius, call Excellent Research, by the project no 23-07722S funded by the Czech Science Foundation and by the project FSI-S-23-8192 funded by the Brno University of Technology. Further, the authors acknowledge the Chemical Processes and Biomaterials research group at the University of West Bohemia in Pilsen, Czech Republic for the preparation of nanofluid.

References

[1] Fiore, M., Sambri, A., Zucchini, R., Giannini, C., Donati, D.M., & De Paolis, M.: Silver-coated megaprosthesis in prevention and treatment of peri-prosthetic infections: a systematic review and meta-analysis about efficacy and toxicity in primary and revision surgery. *European Journal of Orthopaedic Surgery and Traumatology*, vol. 31, no. 3: (2021) pp. 201-220. https://doi.org/10.1007/s00590-020-02779-z

[2] Lex, J.R., Koucheki, R., Stavropoulos, N.A., Di Michele, J., Toor, J.S., Tsoi, K., Ferguson, P.C., Turcotte, R.E., & Papagelopoulos, P.J.: Megaprosthesis anti-bacterial coatings: A comprehensive translational review. (2022).

[3] Cartwright, A., Jackson, K., Morgan, C., Anderson, A., & Britt, D.W.: A review of metal and metal-oxide nanoparticle coating technologies to inhibit agglomeration and increase bioactivity for agricultural applications. (2020).

[4] Kashyap, P.L., Xiang, X., & Heiden, P.: Chitosan nanoparticle-based delivery systems for sustainable agriculture. *International Journal of Biological Macromolecules*, vol. 77: (2015) pp. 36-51. https://doi.org/10.1016/J.IJBIOMAC.2015.02.039

[5] Zhang, A. & Lieber, C.M.: Nano-Bioelectronics. (2016).

[6] Osada, M. & Sasaki, T.: Two-dimensional dielectric nanosheets: Novel nanoelectronics from nanocrystal building blocks. *Advanced Materials*, vol. 24, no. 2: (2012) pp. 210-228. https://doi.org/10.1002/adma.201103241

[7] Blell, R., Lin, X., Lindström, T., Ankerfors, M., Pauly, M., Felix, O., & Decher, G.: Generating in-plane orientational order in multilayer films prepared by spray-assisted layer-by-layer assembly. *ACS Nano*, vol. 11, no. 1: (2017) pp. 84-94. https://doi.org/10.1021/ACSNANO.6B04191

[8] Naber, J.D. & Farrell, P.V.: Hydrodynamics of droplet impingement on a heated surface. (1993).

[9] Mundo, C., Sommerfeld, M., & Tropea, C.: Droplet-wall collisions: Experimental studies of the deformation and breakup process. *International Journal of Multiphase Flow*, vol. 21, no. 2: (1995) pp. 151-173. https://doi.org/10.1016/0301-9322(94)00069-V

[10] Rioboo, R., Tropea, C., & Marengo, M.: Outcomes from a drop impact on solid surfaces. *Atomization and Sprays*, vol. 11, no. 2: (2001) pp. 155-165. https://doi.org/10.1615/atomizspr.v11.i2.40

[11] Tanvir, S. & Qiao, L.: Surface tension of nanofluid-type fuels containing suspended nanomaterials. *Nanoscale Research Letters*, vol. 7, no. 1: (2012) p. 226. https://doi.org/10.1186/1556-276X-7-226

[12] Ennis, B.J., Tardos, G., & Pfeffer, R.: A microlevel-based characterization of granulation phenomena. (1991).

[13] Abberger, T., Seo, A., & Schaefer, T.: The effect of droplet size and powder particle size on the mechanisms of nucleation and growth in fluid bed melt agglomeration.

[14] Rukosuyev, M.V., Barannyk, O., Oshkai, P., & Jun, M.B.G.: Design and application of nanoparticle coating system with decoupled spray generation and deposition control. *Journal of Coatings Technology and Research*, vol. 13, no. 4: (2016) pp. 769-779. https://doi.org/10.1007/S11998-016-9788-2/FIGURES/17

[15] Franke, J., Koutecký, T., Malý, M., Kalina, M., & Koutný, D.: Study of process parameters of the atomizer-based spray gun for the application of a temporary matte coating for 3D scanning purposes. *Materials Chemistry and Physics*, vol. 282: (2022) p. 125950. https://doi.org/10.1016/J.MATCHEMPHYS.2022.125950

[16] McDermott, K. & Oakley, J.G.: Droplet size and distribution of nebulized 3% sodium chloride, albuterol, and epoprostenol by phase Doppler particle analyzer. *Current Therapeutic Research Clinical and Experimental*, vol. 94: (2021) p. 100623. https://doi.org/10.1016/j.curtheres.2021.100623

[17] Asanuma, Y., Faizal, F., Khairunnisa, M.P., & Lenggoro, I.W.: Deagglomeration of spray-dried submicron particles by low-power aqueous sonication. *Advanced Powder Technology*, vol. 33, no. 1: (2022) p. 103543. https://doi.org/10.1016/J.APT.2022.103543

[18] Lang, R.J.: Ultrasonic atomization of liquids. *Journal of the Acoustical Society of America*, vol. 34, no. 1: (1962) pp. 6-8. https://doi.org/10.1121/1.1909020

[19] Hess, D.: Aerosol delivery devices in the treatment of asthma. (PDF). (2008). https://www.researchgate.net/publication/5349250_Aerosol_delivery_devices_in_the_treatment_of_asthma

[20] Malý, M., Moita, A.S., Jedelsky, J., Ribeiro, A.P.C., & Moreira, A.L.N.: Effect of nanoparticles concentration on the characteristics of nanofluid sprays for cooling applications. *Journal of Thermal*

Analysis and Calorimetry, vol. 135, no. 6: (2019) pp. 3375-3386. https://doi.org/10.1007/s10973-018-7444-z
[21] Vafaei, S., Borca-Tasciuc, T., Podowski, M.Z., Purkayastha, A., Ramanath, G., & Ajayan, P.M.: Effect of nanoparticles on sessile droplet contact angle. *Nanotechnology*, vol. 17, no. 10: (2006) pp. 2523-2527. https://doi.org/10.1088/0957-4484/17/10/014
[22] Safiei, W., Rahman, M.M., Yusoff, A.R., & Radin, M.R.: Preparation, stability, and wettability of nanofluid: A review. *Journal of Mechanical Engineering and Sciences*, vol. 14, no. 3: (2020) pp. 7244-7257. https://doi.org/10.15282/JMES.14.3.2020.24.0569